Computing excitons in V-shaped quantum wires including band-structure and dielectric effects : binding energies and polarization anisotropy of the bright A_1, B_1, A_2 excitons

M.A. Dupertuis, D.Y.Oberli, E. Kapon

Institute of Quantum Electronics and Photonics, Swiss Federal Institute of Technology-EPFL
Lausanne 1015, Switzerland, Marc-Andre.Dupertuis@epfl.ch

ABSTRACT

We demonstrate an efficient numerical scheme for the computation of the excitonic optical response of actual GaAs/AlGaAs quantum wire structures including a large set of relevant effects; structural, valence band-mixing, dielectric and many-body effects can be accounted for.

The optical response of excitons within k.p envelope function and Hartree-Fock approximation, are computed with band-mixing effects by stream-lined finite element techniques. The quantum-mechanical effects linked to the wire symmetry are also explicitely taken into account for the first time. A detailed comparison with relevant experimental PLE results is made, and a good agreement is obtained, including polarization anisotropy and binding energies of all bright excitons (A_1, B_1, A_2)

Keywords: Quantum wires, Excitons, Finite elements, Polarization anisotropy, Hartree-Fock.

1 INTRODUCTION

Quantum nanostructures, that is to say very small structures where quantum effects are important, have many potential applications, particularly in semiconductor optical devices. Quantum *wire* (QWR) structures are now attaining excellent quality and have become a very interesting "testbed" for one-dimensional (1D) physics. Photoluminescence excitation (PLE) spectroscopy is a unique probe of the linear optical properties of QWR's revealing in particular a strong polarization anisotropy and many excited subbands in GaAs/AlGaAs V-shaped QWR's [1]. However a detailed analysis of the PLE, because of the interplay of valence-band mixing and the actual QWR non-trivial geometry, requires an extensive modelling effort. Excitonic effects in this frame have been very difficult to obtain, and we are aware of only one non-variationnal work in QWR's including band mixing [2]. Converged full absorption spectra including higher excited subbands, necessary to describe PLE spectra, remain however difficult to obtain, because of the large size of the numerical problem.

We demonstrate here an optimized numerical scheme that allows to compute with moderate resources complete PLE spectra, including also additionnal effects like dielectric effects. With this scheme it will also be possible to follow the evolution of the absorption spectra towards gain with rising carrier density. Such absorption / gain spectra are also essential for the understanding of QWR devices like QWR LED's, lasers and modulators [3], since many-body effects give rise to a significant reduction of oscillator strength at the band-edge in this case [4].

An originality of our work is also that good use is made of the inherent low symmetry of most of the actually grown structures today. A proper group-theoretical classification with well-defined selection rules has been set-up [5], allowing now to refer properly to the bright excitons of a C_s QWR as the A_1, B_1, A_2 excitons, active in the growth, parallel and perpendicular polarizations respectively (Fig.1). In addition the use of symmetry in the computation allows for increased efficiency (memory/time/accuracy).

Some first results are presented for a well-known structure for which excellent PLE spectra and transmission electron micrograph (TEM) pictures are available [1]. The agreement with experimental results, which is now obtained *without any free parameter* is greatly improved and definitely allows us to recognize *more features* in the optical spectra.

2 NUMERICAL APPROACH

The typical V-shape of our QWRs is shown on Fig.1. The contour is directly extracted from a TEM picture with very good accuracy (pen accuracy!). The QWR is quite symmetric, sufficiently enough to use this fact both for calculation and for understanding the resulting selection rules.

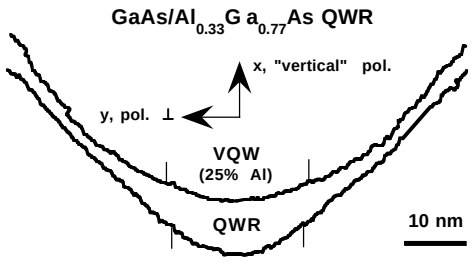

Figure 1: Geometry of the QWR, taken from TEM, (includes the vertical quantum well (VQW))

To obtain the absorption spectra we have chosen to compute first the single-particle band-structure, then the optical and Coulomb matrix elements and finally the optical absorption including the effect of the many-body interaction. This is a three-step approach allowing an easy interpretation of the nature of the numerous peaks appearing in the absorption spectra in terms of single particule subbands, especially useful in the case of strong confinement in quantum wires. All three steps are integrated in the sense that they are directly formulated in Fourier space along the QWR direction and in real space in the other two. Moreover the first two steps use the same finite elements on a common subgrid (the QWR region).

2.1 k.p band-structure

We use a simple effective mass approximation for the electrons, and a four-band Luttinger model for the holes. The details of our properly oriented Luttinger hamiltonian (with respect to the crystal structure) have already been given in [1,5]. To take into account the geometrical shape of the QWR we use the finite element (FE) method which we recommend over various other commonly used approaches (finite differences and orthogonal expansions). Unfortunately these reasons are two long to develop here. A few other authors have also used the FE method in this context.

We show on Fig. 2 the computed valence band-structure corresponding to the profile shown on Fig.1 (C_1 symmetry group, quasi- C_s with one symmetry plane, see [5]). A novelty in Fig.2 is that *k=0* states are classified according to the ZC group [5] and developped into conjugate bands. In the C_s case the (010) quantization direction for spinors allows to enforce in addition well-defined symmetries on each envelope function component [5] (also outside the Gamma point). All the true crossings between $^1E_{1/2}$ and $^2E_{1/2}$ bands of the C_s group become slight anticrossings in Fig.2 because the QWR symmetry is very slightly broken.

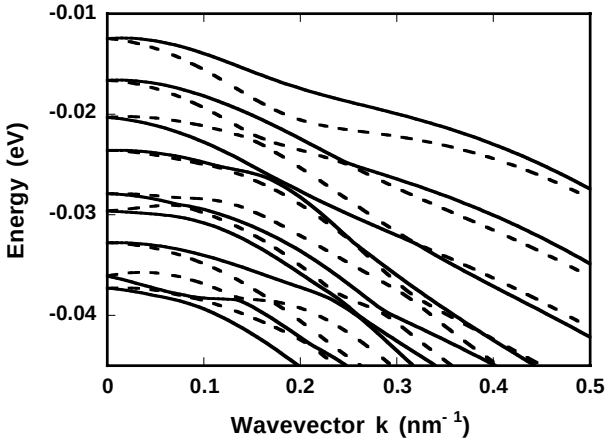

Figure 2: Normal and conjugate bands of the QWR.

The electron subbands (not shown) are quite parabolic and do not show any crossings/ anticrossings.

2.2 Coulomb matrix elements

The second step deals with the computation of the following Coulomb matrix elements. Such matrix elements can be expressed as

$$V^{\sigma_1,\sigma_2,\sigma_3,\sigma_4}_{k-q,k'+q,k',k} = \iint d^2\vec{r}\, d^2\vec{r}' \quad \psi^{\sigma_1\,*}_{k-q}(\vec{r})\, \psi^{\sigma_2\,*}_{k'+q}(\vec{r}')\; G_q(\vec{r},\vec{r}')\; \psi^{\sigma_3}_{k'}(\vec{r}')\, \psi^{\sigma_4}_{k}(\vec{r}) \tag{1}$$

where the wavefunctions have been calculated during the first step. Dielectric effects, which have been shown to be important as soon as a detailed comparison is required (already in quantum wells [6]), have already been studied by few authors [5,7]. They are included here by requiring that $G_q(r,r')$ is not the simple 1D-FT of the $1/(\varepsilon r)$ bulk interparticle Coulomb potential, but the solution of the following Poisson equation:

$$\left[\vec{\nabla}\left(\varepsilon(\vec{r})\vec{\nabla}\right) - q^2\varepsilon(\vec{r})\right] G_q\left(\vec{r},\vec{r}'\right) = -4\pi\delta\left(\vec{r}-\vec{r}'\right) \tag{2}$$

As we need to calculate a large number of Coulomb matrix elements (here $\sim 10^7$, each of them being the 4-dimensional spatial integral of Eq.(1)!) it is essential to efficiently streamline (and intrinsically parallelize) their computation. This is done in the following way. The Poisson operator (2) is discretized with the same FEs on a large circular grid (typically 130 nm radius) *extending* the first QWR grid and is LU-decomposed *only once* for every value of q (the momentum transfer). Instead of solving for the Green function of the Coulomb problem we collect all the required products of wavefunctions as a large set of right hand sides (RHSs) which can be solved in parallel using the LU decomposition. This procedure leads to a set of solutions that can be interpreted as the Coulomb potential generated by the set of wavefunction products involving *r'* in (2) (these products may become complex for a non-real hamiltonian!). Finally a large rectangular matrix-matrix multiplication with the original set of RHS wavefunction products (performed on the smaller QWR grid only) leads in one step all the possible respective Coulomb matrix elements.

The advantages of this direct algorithm are numerous: 1) it is intrinsically parallellized and optimized routines like widespread BLAS/LAPACK can be used throughout, 2) the Poisson problem is banded and easy to treat, 3) the spatial variation of the dielectric constant is trivial to take into account, 4) it is easy to rise up the order of the finite-elements and gain in accuracy/time (as from trapezoidal to Simpson inetgration), 5) explicit integrations are avoided, 6) no need to insert costy numerical interpolations.

Special care must however be paid to the slowly decreasing Coulomb potentials at the outer border of the

large grid. For each RHS we enforced the correct asymptotic behavior via the Dirichlet boundary value set by the product of the respective "integrated effective RHS charge" and a typical q-dependent "asymptotic" value. The former is computed over the QWR grid using the mass matrix, and is not necessarily equal to the electron charge (e.g. it is zero in the case of an odd wavefunction product). The latter have been consistently chosen to correspond *to the 1D-Discrete Fourier Transformation (DFT) of the asymptotic 1/r Coulomb potential at the finite large radius of the outer grid*. We took care to remain fully consistent in k-space in the sense of the DFT. This is because with a normal FT (or a Fourier series) the q-dependent Coulomb matrix elements diverge when q tends to zero whilst in the DFT they remain *finite at q=0*. When the k-discretization is refined the DFT diverges *consistently* but it is never needed to refine the discretization beyond a scale set by the exciton radius, so the procedure is practical. This last point is extremely simple to implement.

2.3 Absorption spectra

To compute the optical absorption one then needs to get all the microscopic polarizations corresponding to the quantum expectation values $p_k^{s,t} = \left\langle \hat{b}_{-k}^t \hat{a}_k^s \right\rangle$ (see [8]).

For a weak stationnary light field probing the linear optical absorption the microscopic polarization obey a large set of linear equations with three inhomogeneous RHS (proportional to the dipole matrix elements) corresponding to possible linear light polarizations (for more details see [8]). This large set must be repeatedly solved for every value of frequency to get a full linear absorption spectra. The following procedure provided nearly two orders of magnitude with respect to a sequence of direct solutions: 1) solve the first spectral point with a direct method, 2) for the subsequent point inject the previous solution in an *iterative* solver (preconditioned conjugate gradient).

Symmetrized Hartree-Fock terms linear in density have also been easily implemented in this scheme [8] and will allow a future study of high-density 1D plasmas.

2.4 Implementation and performance

Our code is written is Fortran 90, calling only fairly standard libraries (BLAS, LAPACK, ARPACK, NAG, Numerical Recipes). Presently only simple linear basis functions on a set (n_x x n_y) of irregular quadrilateral finite elements are implemented.

We use the following numerical parameters: 6 electron and 8 hole subbands are taken into account. The real space n_x x n_y grid is 28 x 80 and adapted to the TEM picture of the full QWR (10 intervals span the QWR thickness, the lateral width is 63 nm). In k-space 26 intervals up to 0.5 nm^{-1} are used. The banded eigenproblem is 2240 x 57 for electrons, and 8532 x 231 for holes. The Poisson grid involves 6549 nodes in a circle of radius 130 nm. The Coulomb matrix rank is 4452 and solved 1200 times (three polarization-dependent absorption spectra, each 400 points). Here slight departures from perfect symmetry were taken into account, however they do not result in any significant effect in the absorption spectra (the results will be interpreted as if mirror symmetry was perfect). A consequence is that the performances can be further raised by a factor 3-4 when using symmetry (used in extensive parametric studies).

For this typical problem size the total memory needed is < 550 MB at any time during the computation (about 1/3 could still easily be gained). The CPU time requirements are: 1) band-structure: ~7 min., 2) Coulomb matrix elements: ~6.25 hours, 3) absorption spectrum: <3 hours.

These figures were obtained on an old Unix DEC-Alpha Workstation. On a modern MacIntosh G4 Laptop (500 MHz, OS-X, Absoft compiler) the time requirements are only twice, for an undisturbing background computation.

3 OPTICAL SPECTROSCOPY

Our main goal is to interpret in detail high quality optical PLE spectra like shown in Fig.3 (8.8 nm thick QWR of Fig.1, called "2.5 nm nominal" in [1b]). Such spectra have not been ever compared with a calculation incorporating both band-mixing and the Coulomb interaction. Dipolar matrix elements were first used to understand them [1], then further free-carrier (FC-) optical spectra (i.e. without Coulomb, but with full VB non-parabolicity and k-dependent matrix elements) [9].

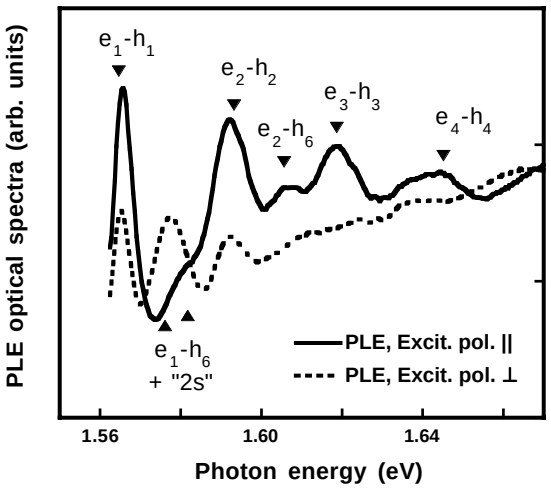

Figure 3: Experimental PLE spectra of the QWR. The triangles correspond to the calculated peaks (Fig.4).

On Fig.4 we display the calculated excitonic spectra and on Fig.5 the corresponding FC-spectra (exactly same parameters). In both cases the homogeneous broadening was deliberately kept quite small (3 meV HWHM), in order to be able to identify spectroscopic details. We should stress that these calculated spectra *do not involve any free physical parameters* (all parameters are given in Ref. [1b]).

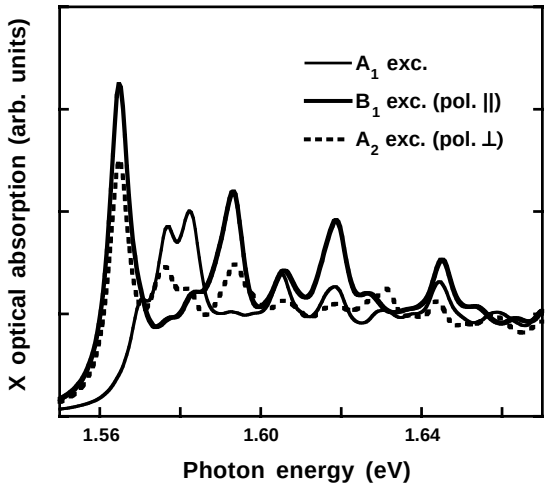

Figure 4: Calculated absorption with excitonic effects.

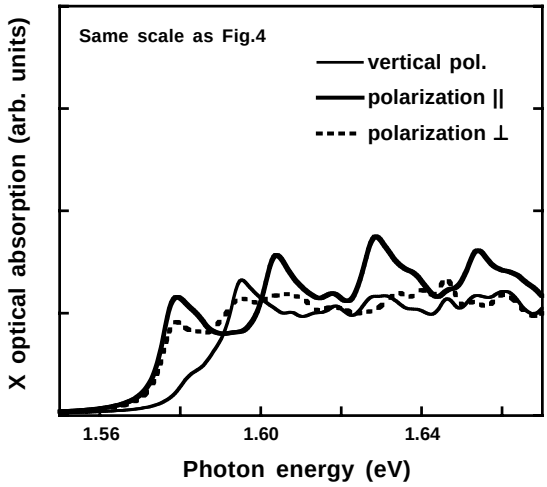

Figure 5: Calculated absorption without excitonic effects (same parameters as in Fig.4).

Many features of Fig.3 are accounted for in Fig.4: 1) a rigid excitonic energy shifts was previously introduced as the only ad-hoc free parameter [1,9], it is now unnecessary and the e1-h1 binding energy can be estimated to be 14.5 meV, of the order of 4 times the bulk Rydberg (the ideal 2D value), 2) the sequence of oscillator strengths (affected by excitonic enhancement) is much closer to the experiments than the FC spectra, including the polarization anisotropy (especially the flattening above e2-h2 in perpendicular polarization (A_2 exciton)), 3) The typical high energy tail of each peak in Fig.5 (1D density of states effect) is suppressed in agreement with Fig.3, 4) the weaker peak in parallel polarisation (B_1 exciton) between the e2-h2 and e3-h3 transitions that was not yet identified is now attributed to an e2-h6 non-diagonal transition, 5) The peak between e1-h1 and e2-h2 which was identified as a light-hole-like e1-h6 transition in Fig.3 and 5 appears now to be composed of two narrower peaks in Fig.4. The wider spectral width in Fig.3 and its average position let us conjecture that two peaks may indeed be resolved in samples with reduced inhomogeneous broadening. Since only a single peak appears in the FC-spectra (also in the dipolar matrix element spectra) a further analysis is required to check whether one of the two peak can be attributed to a "2s-like" resonance ("2s-like": because there is no rotationnal symmetry) of the e1-h1 excitons.

Three other remarks are worth making: 1) the e1-h2 first peak in the A_1 exciton spectrum is also enhanced by excitonic correlations and compares now better with [10], 2) Varying the number of subbands demonstrate that the transfer of oscillator strength from higher subbands to the lowest optical transitions is quite important, 3) the ratio of the subband separation e1-h1/e2-h2 is slightly larger in the calculation by a few meV (see Figs.3,4). This interesting discrepancy needs to be investigated further.

4 CONCLUSIONS

The development of a large code solving for excitons in quantum wires has certainly been a rewarding undertaking which allowed to improve our understanding of the complex optical spectra of QWRs. We have also addressed computationnal efficiency issues (memory/ time/ accuracy).

Still more work must be done to reach in QWRs the status of the best excitonic calculations made in quantum wells [6,11]. In addition to adding more bands and converge even better in k-space we plan to include in the near future the self-energy terms linked with image charges, as well as the non-parabolicity of the conduction band. These effects all start to become important at the level of detailed comparison now pursued. We also plan to investigate the polarization-dependent Hartree-Fock terms that are linear in density in continuing studies. From the computational point of view second order finite elements will be worth introducing.

REFERENCES

[1] F.Vouilloz et al., Phys.Rev.Lett.**78**, p.1580 (1997); ibid. Phys.Rev.B**57**, p.12378 (1998)

[2] A.Siarkos, E.Runge, Phys.Rev.B**61**, p.16854 (2000)

[3] H. Weman et al., Appl.Phys.Lett.**79**, p.4 (2001)

[4] F.Rossi, G.Goldoni, O.Mauritz, E.Molinari, J.Phys. : Condens.Matter **11**, 5969 (1999)

[5] M.-A.Dupertuis et al., Europhys.Lett.**52**, p.420 (2000)

[6] L.C.Andreani, A.Pasquarello, Phys.Rev.B**42**, p.8928 (1990)

[7] see e.g. E.A.Muljarov et al., Phys.Rev.B**51**, p.14370 (1995) and references therein.

[8] M.A.Dupertuis, Phys. Stat. Sol.(a) **221**, p.323 (2000)

[9] M.A.Dupertuis et al., Physica E **2**, p.940 (1998)

[10] E.Martinet et al., Phys. Stat. Sol.(a) **178,** p.233 (2000).

[11] R. Winkler, Phys. Rev. B 51, p.14395 (1995).